

Highly Parallel Magnetic Tweezers by Targeted DNA Tethering

Iwijn De Vlaminck,[†] Thomas Henighan,[†] Marijn T.J. van Loenhout,[†] Indriati Pfeiffer,[‡] Julius Huijts,[†] Jacob W.J. Kerssemakers,[†] Allard J. Katan,[†] Anja van Langen-Suurling,[†] Emile van der Drift,[†] Claire Wyman,^{‡,§} and Cees Dekker^{*,†}

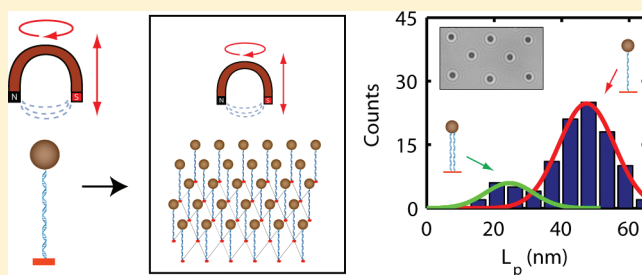
[†]Kavli Institute of Nanoscience, Delft University of Technology, Delft, Lorentzweg 1, 2628 CJ, The Netherlands

[‡]Department of Cell Biology and Genetics, Cancer Genomic Center, [§]Department of Radiation Oncology, Erasmus MC, P.O. Box 2040, 3000 CA Rotterdam, The Netherlands

S Supporting Information

ABSTRACT: Single-molecule force-spectroscopy methods such as magnetic and optical tweezers have emerged as powerful tools for the detailed study of biomechanical aspects of DNA-enzyme interactions. As typically only a single molecule of DNA is addressed in an individual experiment, these methods suffer from a low data throughput. Here, we report a novel method for targeted, nonrandom immobilization of DNA-tethered magnetic beads in regular arrays through microcontact printing of DNA end-binding labels. We show that the increase in density due to the arrangement of DNA-bead tethers in regular arrays can give rise to a one-order-of-magnitude improvement in data-throughput in magnetic tweezers experiments. We demonstrate the applicability of this technique in tweezers experiments where up to 450 beads are simultaneously tracked in parallel, yielding statistical data on the mechanics of DNA for 357 molecules from a single experimental run. Our technique paves the way for kilo-molecule force spectroscopy experiments, enabling the study of rare events in DNA–protein interactions and the acquisition of large statistical data sets from individual experimental runs.

KEYWORDS: Magnetic tweezers, single-molecule force spectroscopy, microcontact printing, increased packing density



Magnetic tweezers (MT) have become a widely used single-molecule technique for the study of the mechanics of macromolecules and the dynamics of enzymes that act on DNA or RNA.¹ The popularity of the MT technique is due to its low cost, simplicity of implementation, and the possibility to monitor and control the effects of torsional and tensional stress on enzyme–DNA interactions.^{2–4} In magnetic tweezers, a DNA molecule is tethered between a paramagnetic bead and the surface of a flow cell. An external magnet exerts a force and torque on the DNA molecule (see Figure 1a for a schematic).¹ The length of the DNA molecule is measured by tracking the XYZ position of the paramagnetic bead using video microscopy, providing a means for monitoring, for example, enzyme-induced changes in DNA topology. The force and torque exerted on the molecule can be extracted from measurements of the position and thermomechanical noise spectrum of the motion of the bead.^{1,4}

In standard MT experiments, only a single molecule of DNA is addressed in an individual experiment. Since several paramagnetic beads can be captured in the imaging field of view, MT inherently bear potential for multiplexing,^{5–7} thereby increasing the data throughput in single-molecule force–spectroscopy experiments. The achievable data throughput in multiplexed magnetic tweezers is limited by the density of isolated and trackable beads in the field of view. Here, we show that it is possible to fabricate regular arrays of closely spaced DNA-bead tethers, thus increasing the density of trackable beads in the field of view by up to 1

order of magnitude. We create such regular arrays of surface-immobilized tethers through microcontact printing of a pattern of DNA-end-binding labels on the surface of a flow cell (see scheme in Figure 1). The use of microcontact printing in this context is particularly advantageous as it offers a facile, cheap, and robust method for the fabrication of sub-100 nm protein structures.⁸ A lipid bilayer serves as a highly inert surface passivation layer that prevents nonspecific binding of the magnetic beads.

In the standard MT approach, DNA molecules are immobilized on a surface that is randomly covered with DNA-end-binding labels, leading to a sparse, random distribution of DNA-tethered beads. Following this procedure, DNA-tethered beads can only be used for further experimenting and analysis if they are spaced farther than an experiment-specific distance d_0 from their nearest neighbor. This requirement for a minimum bead-to-bead distance results from crosstalk in position tracking when the diffraction pattern of the beads overlaps and from attractive forces that arise between neighboring beads as a result of magnetic dipole–dipole coupling that can lead to irreversible pull-in of DNA-tethered beads. The minimum separation thus depends on the size of the defocused bead image as well as the length of the DNA tethers.

Received: September 21, 2011

Revised: October 17, 2011

Published: October 21, 2011

The maximum achievable number of useful DNA-tethered beads can be calculated from the probability density of finding the nearest neighbor at some given distance r . For point-like particles that are randomly distributed on a 2D plane, the probability density reads⁹

$$\omega(r) = 2\rho\pi r e^{-\rho\pi r^2} \quad (1)$$

with ρ as the surface density of DNA-tethered beads. The number of productive tethers (i.e., those with $r > d_0$) can therefore be calculated as

$$N_{\text{bead}} = A_{\text{FOV}} \rho \int_{d_0}^{\infty} \omega(r) dr = A_{\text{FOV}} \rho e^{-\rho\pi d_0^2} \quad (2)$$

with A_{FOV} the area of the field of view. The optimal density that can be achieved is obtained for $dN/d\rho = 0$, yielding a maximum number

of beads of

$$N_{\text{max}} = \frac{A_{\text{FOV}}}{d_0^2} \frac{1}{\pi e} \quad (3)$$

A regular distribution of beads results in a much higher stacking density. Full occupation of a square array pattern with pitch $d = d_0$ yields a surface density $N_{\text{max}} = A_{\text{FOV}}/d_0^2$. For a hexagonal pattern with the same pitch, $N_{\text{max}} = (2/\sqrt{3})(A_{\text{FOV}}/d_0^2)$. Regular arrays can thus lead to an improvement in surface density compared to the case of a random distribution with a factor of πe and $(2/\sqrt{3})\pi e$ (≈ 10) for a square and hexagonal pattern, respectively.

Here, we create regular arrays of DNA-tethered magnetic beads via surface patterning of antidigoxigenin protein, which specifically binds to a digoxigenin end-labeled DNA. The protein pattern is prepared via microcontact printing. The protocol for microcontact printing is described in Figure 2a. A negative image of the desired protein pattern is created in a silicon template using a combination of electron-beam lithography and dry etching. Figure 2b shows a scanning electron micrograph of a resulting ~ 100 nm deep square etch pit in silicon. Before (re)use of the silicon template, organic residues are removed from the template (Piranha $\text{H}_2\text{SO}_4/\text{H}_2\text{O}_2$ 3:1, 10 min), and the silicon template is subsequently O_2 -plasma treated to make the surface hydrophilic. A disposable, elastomeric stamp with a flat print surface is cut from a precast PDMS layer (Sylgard 184, Dow Corning) and inked with an antidigoxigenin solution (0.5 mg/mL in PBS buffer, 10 mM). After incubation (30 min), the solution is washed off and the surface-adsorbed layer of antidigoxigenin is transferred to the silicon template. A positive image of the desired protein pattern remains on the PDMS stamp. The pattern on the PDMS stamp is subsequently transferred to a glass slide through microcontact printing. For further details on the latter, see Coyer et al.⁸ Prior to printing, the glass slide is cleaned and treated with a TL1 solution ($\text{NH}_4\text{OH}/\text{H}_2\text{O}_2$, 3:1) to make the surface hydrophilic.

Figure 2c shows an atomic force microscopy (AFM) image of a square antidigoxigenin patch printed on a glass slide. The AFM scan shows that the conformation of the square defined in the

Figure 1. Principle of magnetic tweezers (MT) and increase in data throughput via parallelization. (a) Positioning and rotation of an external magnet allow applying tensional and torsional stress to a DNA-molecule bound to a paramagnetic bead. (b) Regular arrays of DNA-tethered beads greatly increase the achievable data-throughput. (c) Schematic outline of multiplexed MT. Bead arrays in a flow cell (FC) are visualized using a microscope system, consisting of an LED, a lens (L), an objective (OBJ), and a camera. The XYZ positions of the magnetic beads are measured via video microscopy.

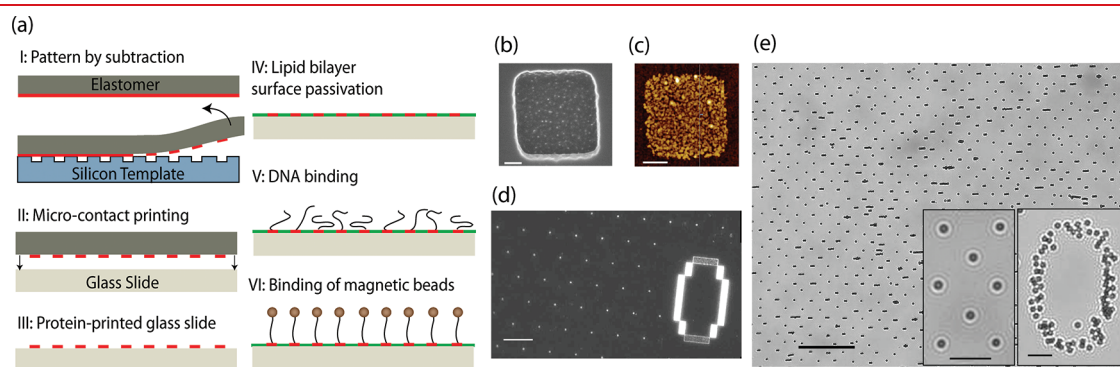


Figure 2. Protocol for making regular arrays of DNA-bead tethers and characterization. (a) A protein layer on a PDMS stamp is transferred onto a prefabricated silicon template (panel I). The protein pattern that remains on the elastomer is subsequently transferred to a glass slide (panel II–III). The nonprinted area is passivated using a lipid bilayer to prevent nonspecific binding of DNA or beads to the surface (panel IV). Digoxigenin-end-labeled DNA is bound to the protein patches (panel V). Streptavidin-coated superparamagnetic beads subsequently bind to the DNA (panel VI). (b) Scanning electron micrograph of an etch pit in the silicon template, corresponding to panel I in a (scale bar 100 nm). (c) AFM scan of an antidigoxigenin patch printed on glass, corresponding to panel III in a (scale bar 200 nm, total height scale 10 nm). (d) Fluorescence microscopy images of a hexagonal pattern (pitch, $d_0 = 9 \mu\text{m}$) of rhodamine-labeled antidigoxigenin patches (left) and a number marker on the sample (right) (scale bar $10 \mu\text{m}$). (e) Zoom (40%) of a field of view ($300 \mu\text{m} \times 400 \mu\text{m}$) in which 996 magnetic beads and bead clusters are organized in a square array ($d_0 = 9 \mu\text{m}$, scale bar $40 \mu\text{m}$). A total of 787 trackable, spatially isolated beads were found. The insets show a zoom-in on eight beads organized in a square array DNA-bead tethers bound and a number marker on the sample (scale bars $10 \mu\text{m}$).

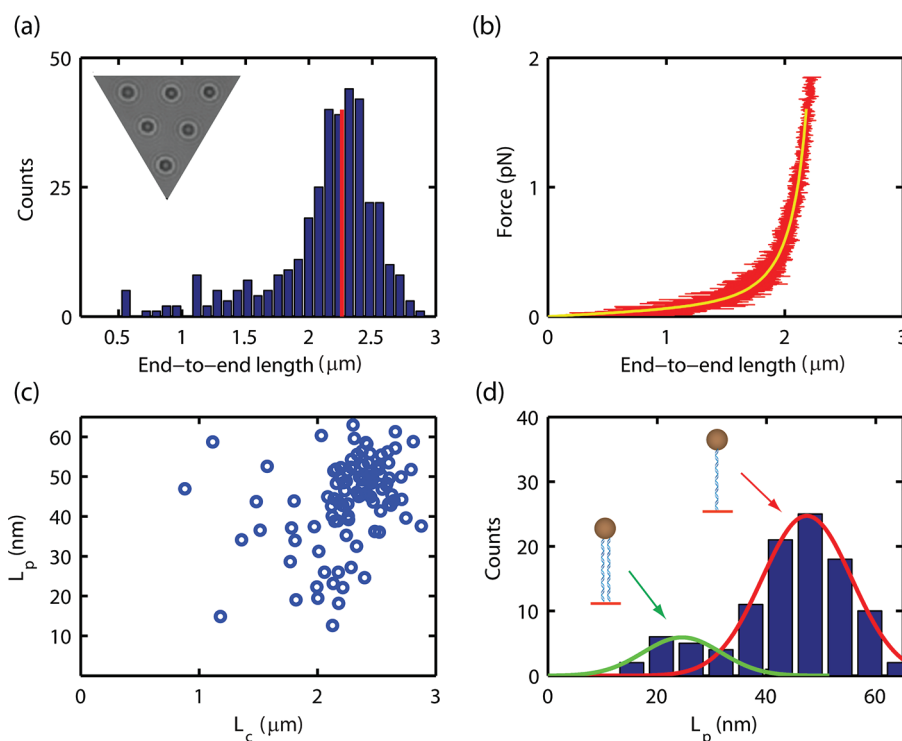


Figure 3. Highly parallel measurement and analysis of DNA mechanics. (a) Histogram of the measured bead height measured for a 7.3 kb dsDNA at a nominal force of 1.8 pN. $N_{\text{bead}} = 450$ beads were found in a hexagonal pattern with a pitch of $15 \mu\text{m}$ (a fragment of such pattern is shown in the inset). Eighty percent ($N_{\text{mol}} = 357$) of these DNA-bead tethers were found to have an end-to-end distance longer than $0.5 \mu\text{m}$. Red line indicates the expected length. (b) Example of a force response curve measured for a single DNA-bead tether in the array. (c) Scatter plot of the persistence length, L_p , and contour length, L_c , extracted by fitting a wormlike chain model to the force response of an ensemble of DNA-bead tethers ($N_{\text{bead}} = 250$). (d) Histogram of extracted L_p for $N_{\text{mol}} = 105$. Two peaks are found, centered around $L_p = 48 \text{ nm}$ and $L_p = 25 \text{ nm}$, corresponding to single and double tethered molecules, respectively.¹³

silicon master is excellently reproduced. The protein patch has a rough surface with median peak height of $\sim 4 \text{ nm}$, consistent with a high coverage of a monolayer of printed protein, thereby confirming observations in ref 8. Figure 2d shows images of a hexagonal pattern of fluorescently labeled antidigoxigenin square patches (each 200 nm) printed on a glass slide. The image reveals a regularly spaced and uniformly occupied array of fluorescent protein patches ($d_0 = 9 \mu\text{m}$).

After microcontact printing of the glass slide, a flow cell for MT experiments is prepared with the protein-printed slide as the bottom layer. In our experiments, protein patterns with a patch size in the range of 200 to 600 nm and pitch in the range of 9 to $20 \mu\text{m}$ are used. The size of the active, DNA-binding area in the resulting pattern is thus only a 10^{-2} to 10^{-4} fraction of the total area. This places a strong requirement on the ratio between DNA-specific binding and random nonspecific binding of DNA or beads to the surface ($>10^3$ to 10^5).

To meet this requirement, a highly inert lipid bilayer is formed in the area between the protein patches in order to prevent nonspecific DNA and bead binding.¹⁰ To this end, 50 nm lipid vesicles were prepared as described previously¹¹ and suspended in a buffer (10 mM Tris, 100 mM NaCl (pH 8)). A lipid bilayer spontaneously assembles on the protein-free part of the surface upon adsorption and spontaneous rupture of the lipid vesicles (30 min). After surface passivation, double-stranded (ds)DNA molecules (7.3 kb , 500 pM) were introduced into the flow cell (buffer: Tris-HCl (pH 7.8), 100 mM NaCl, 4 mM MgCl_2). DNA molecules were prepared as described previously.¹² The DNA is

digoxigenin labeled at one end to allow specific binding to the antidigoxigenin patches on the surface, and a biotin label on the other end allows subsequent attachment of streptavidin-coated paramagnetic beads (for more details on the preparation of this 7.3 kb dsDNA construct, see ref 12.). After incubation (10 min), free DNA was removed from the flow cell and $1 \mu\text{m}$ streptavidin-coated paramagnetic beads (MyOne, Invitrogen) are introduced and allowed to settle on the surface (10 min). After removal of nonbound magnetic beads, a regular pattern of surface-tethered magnetic beads remains.

Figure 2e shows an example of a square pattern of DNA-tethered magnetic beads of $1 \mu\text{m}$ diameter. The image shows a zoom (40%) of a $300 \times 400 \mu\text{m}$ field of view in which 996 magnetic beads and bead clusters are organized in a square array. In this field of view, 787 spatially isolated beads were found (using an automated bead-finding procedure, see Supporting Information), that is, a factor of 4.8 more than can be achieved using a random distribution of tethers (see eq 3). An alternative protocol where DNA is first incubated with the magnetic beads and where DNA-bound beads are subsequently introduced in the flow cell yielded similar results (data not shown). Furthermore, backfilling of nonfully occupied arrays is possible through the addition of DNA-bound beads. In following this procedure, binding of DNA-tethered beads to an already occupied protein patch is prevented through steric hindrance (for attachment pads smaller than the bead diameter). As a result, the Poisson limit on the fraction of patches occupied with a single molecule can be overcome.

The above-described microcontact printing based method allows the facile and robust preparation of dense regular arrays of DNA-bead tethers for multiplexed magnetic tweezers with minimal extra processing steps and time required for sample preparation. Particularly advantageous in this context is that the silicon master template, with e-beam defined nanostructures, can be reused to prepare many flow cells, thereby significantly reducing the sample cost. We found that >10 flow cells can reproducibly be prepared by reusing the same master template without noticeable degradation in sample quality.

To demonstrate the potential of extracting large statistically meaningful data sets out of a single experimental run by means of these highly parallel magnetic tweezers, we have measured and analyzed the mechanical properties of an ensemble of 7.3 kb dsDNA. The magnetic tweezers setup used in this work consists of a microscope imaging system with $25\times$ optical magnification and a 1.4 megapixel camera (Falcon1.4M, Dalsa) resulting in a $300 \times 400 \mu\text{m}$ field of view. Modeling of the force fields generated by the magnet configuration used in this work indicates that the force-variation in the field of view is smaller than 1% in the force range used in the experiments (data not shown). To address the computational challenge of accurate positional tracking of all the magnetic beads in the field of view, we store images acquired by the camera on a hard drive and perform an image analysis offline after the experiment.⁵

A flow cell was prepared with a hexagonal pattern of anti-digoxigenin patches ($d_0 = 15 \mu\text{m}$). A total of 450 beads were found in the field of view using an automated procedure (Supporting Information). Figure 3a shows a histogram of the maximum bead height measured during 25 s at a nominal force of $F_{\text{mag}} = 1.8 \text{ pN}$ in a 10 mM Tris buffer (pH 7.5). Out of 450 beads in the field of view, 80% (357) of the DNA-bead tethers displayed an end-to-end distance longer than $0.5 \mu\text{m}$. The histogram of the measured lengths shows a most probable length of $2.31 \pm 0.08 \mu\text{m}$, close to the expected length $= 2.26 \pm 0.005 \mu\text{m}$ (at $F_{\text{mag}} = 1.8 \text{ pN}$, 25 s measurement time). Several experimental factors contribute to the observed distribution in end-to-end distances (1) the random distribution of the positions of attachment of DNA on the bead, (2) errors made in determining the position of the surface of the flow cell, (3) the variation in the conformation of attachment of the DNA-end-binding labels, and last (4) a variation in the number of DNA molecules bound to a single bead (see below).

In the next experiment, we performed a high-throughput analysis of the elastic response of a large set of DNA tethers. Figure 3b shows a measurement of the characteristic elastic response of dsDNA. The force required to extend a dsDNA molecule, thereby reducing the conformational entropy of the molecule, is well described by a wormlike chain (WLC) model.^{13,14} The model has two parameters, the contour length of the molecule, L_c , and the persistence length, L_p , a measure for the length scale over which orientational fluctuations decay. dsDNA has a well-defined L_c of 0.34 nm per base pair ($2.48 \mu\text{m}$ for 7.3 kb).¹³ L_p is modestly dependent on salt and was measured to be $L_p \approx 50 \text{ nm}$ in the range of 30 mM to 150 mM Na^+ .¹³ In single-molecule pulling experiments, the extracted L_p values furthermore depend on the length of the molecule for short DNA substrates and are affected by degrees of freedom of bead fluctuations.¹⁵ We used the dynamic force spectroscopy method proposed by Kruithof et al. for the fast and accurate analysis of the DNA force response.¹⁶ The total time required for the experimental run was only 8 min (including measurements of the force response and calibration

measurements of a bead-specific height-offset and a force calibration factor). Figure 3c shows a scatter plot of the extracted L_p and L_c values for 105 molecules. Figure 3d shows the distribution of the extracted L_p . Two peaks are easily distinguished and are centered around $L_p = 48 \text{ nm}$ and $L_p = 25 \text{ nm}$, corresponding to singly tethered and doubly tethered beads respectively.¹⁷

The highly parallel magnetic tweezers technique used here will be highly useful in the systematic study of the mechanical properties of ssDNA, RNAs and protein-bound DNAs.¹⁸ DNA-binding proteins can significantly alter the mechanical parameters of the DNA, and high-throughput measurements of these parameters can yield crucial insight into protein function.^{3,12}

In conclusion, we have described a new method for the targeted surface-attachment of DNA-bead tethers via microcontact printing of DNA-end-binding labels. DNA tethering in a regular array can yield a one-order-of-magnitude increase in the density of DNA-tethered beads on the surface, thereby greatly increasing the data throughput in magnetic tweezers experiments. Similar improvements in throughput can be realized for tethered-particle-motion experiments, holographic optical tweezers experiments and, experiments with torque-sensitive magnetic tweezers.^{4,19,20} To illustrate the potential of this technique in providing a high-throughput analysis in magnetic tweezers, we performed measurements of the mechanical parameters of up to 357 dsDNA molecules in a single experimental run. Further advances can be made by increasing the image field-of-view size, for example, by making use of a larger camera that leads to an increase of the field-of-view size without compromising the tracking accuracy.⁵

The method presented here paves the way for kilo-molecule level magnetic tweezers experiments. Kilo-molecule magnetic tweezers will greatly facilitate the force and torque spectroscopy studies of DNA–protein and RNA–protein interactions through the acquisition of large statistical data sets from individual experimental runs.

■ ASSOCIATED CONTENT

Supporting Information. Additional information and figures. This material is available free of charge via the Internet at <http://pubs.acs.org>.

■ AUTHOR INFORMATION

Corresponding Author

*E-mail: c.dekker@tudelft.nl.

■ ACKNOWLEDGMENT

We thank Susanne Hage for technical assistance. This work was supported by a “DNA-in-action” grant from the “Stichting voor Fundamenteel Onderzoek der Materie (FOM)”, which is financially supported by the “Nederlandse Organisatie voor Wetenschappelijk Onderzoek (NWO)”, and a VICI grant (C.W. laboratory) from the Chemical Science Division of NWO. T.H. thanks The Netherlands-America Fulbright Foundation for their support.

■ REFERENCES

- (1) Strick, T. R.; et al. *Rep. Prog. Phys.* **2003**, *66*, 1.
- (2) Koster, D. A.; Croquette, V.; Dekker, C.; Shuman, S.; Dekker, N. H. *Nature* **2005**, *434*, 671.

- (3) De Vlaminck, I.; Vidic, I.; van Loenhout, M. T. J.; Kanaar, R.; Lebbink, J. H. G.; Dekker, C. *Nucleic Acids Res.* **2010**, *38* (12), 4133.
- (4) Lipfert, J.; Kerssemakers, J. W. J.; Jager, T.; Dekker, N. H. *Nat. Methods* **2010**, *7*, 977.
- (5) van Loenhout, M. T. J.; Kerssemakers, J. W. J.; De Vlaminck, I.; Dekker, C., unpublished work.
- (6) Ribbeck, N.; Saleh, O. A. *Rev. Sci. Instrum.* **2008**, *79*, 094301.
- (7) Assi, F.; Jenks, R.; Yang, J.; Love, C.; Prentiss, M. J. *Appl. Phys.* **2002**, *92*, 5584.
- (8) Coyer, S. R.; García, A. J.; Delamarche, E. *Angew. Chem., Int. Ed.* **2007**, *46*, 6837.
- (9) Torquato, S.; Lu, B.; Rubinstein, J. *Phys. Rev. A* **1990**, *41*, 2059.
- (10) Svedhem, S.; Pfeiffer, I.; Larsson, C.; Wingren, C.; Borrebaeck, C.; Höök, F. *ChemBioChem* **2003**, *4*, 339.
- (11) Barenholz, Y.; Gibbes, D.; Litman, B. J.; Goll, J.; Thompson, T. E.; Carlson, F. D. *Biochemistry* **1977**, *16*, 2806.
- (12) van Loenhout, M. T. J.; van der Heijden, T.; Kanaar, R.; Wyman, C.; Dekker, C. *Nucleic Acids Res.* **2009**, *37*, 4089.
- (13) Marko, J. F.; Siggia, E. D. *Macromolecules* **1995**, *28*, 8759.
- (14) Bustamante, C.; Marko, J.; Siggia, E.; Smith, S. *Science* **1994**, *265*, 1599.
- (15) Seol, Y.; Li, J.; Nelson, P. C.; Perkins, T. T.; Betterton, M. *Biophys. J.* **2007**, *93*, 4360.
- (16) Kruithof, M.; Chien, F.; de Jager, M.; van Noort, J. *Biophys. J.* **2008**, *94*, 2343.
- (17) Charvin, G.; Vologodskii, A.; Bensimon, D.; Croquette, V. *Biophys. J.* **2005**, *88*, 4124.
- (18) Yan, J.; Marko, J. F. *Phys. Rev. E* **2003**, *68*, 011905.
- (19) Gelles, J.; Schnapp, B. J.; Sheetz, M. P. *Nature* **1988**, *331*, 450.
- (20) Lipfert, J.; Wiggan, M.; Kerssemakers, J. W. J.; Pedaci, F.; Dekker, N. H. *Nat. Commun.* **2011**, *2*, 439.